Dititanium-Containing 19-Tungstodiarsenate(III) [Ti$_2$(OH)$_2$As$_2$W$_{19}$O$_{67}$(H$_2$O)]$^{8-}$: Synthesis, Structure, Electrochemistry, and Oxidation Catalysis

Firasat Hussain,[a, d] **Bassem S. Bassil,**[a] **Ulrich Kortz,***[a] **Oxana A. Kholdeeva,***[b] **Maria N. Timofeeva,**[b] **Pedro de Oliveira,**[c] **Bineta Keita,**[c] **and Louis Nadjo***[c]

Abstract: The dititanium-containing 19-tungstodiarsenate(III) [Ti$_2$(OH)$_2$As$_2$W$_{19}$O$_{67}$(H$_2$O)]$^{8-}$ (**1**) has been synthesized and characterized by IR, TGA, elemental analysis, electrochemistry, and catalytic studies. Single-crystal X-ray analysis was carried out on Cs$_8$[Ti$_2$(OH)$_2$As$_2$W$_{19}$O$_{67}$(H$_2$O)]·2CsCl·12H$_2$O (Cs-**1**), which crystallizes in the monoclinic system, space group $P2_1/m$, with $a =$ 12.7764(19), $b = 19.425(3)$, $c = $ 18.149(3) Å, $\beta = 110.234(3)°$, and $Z = 2$. Polyanion **1** comprises two (B-α-As^{III}W$_9$O$_{33}$) Keggin moieties linked through an octahedral {WO$_5$(H$_2$O)} fragment and two unprecedented square-pyramidal {TiO$_4$(OH)} groups, leading to a sandwich-type structure with nominal C_{2v} symmetry. Synthesis of **1** was accomplished by reaction of

TiOSO$_4$ and K$_{14}$[As$_2$W$_{19}$O$_{67}$(H$_2$O)] in a 2:1 molar ratio in aqueous, acidic medium (pH 2). Polyanion **1** could also be isolated as a tetra-n-butyl ammonium (TBA) salt, {(n-C$_4$H$_9$)$_4$N}$_5$H$_3$-[Ti$_2$(OH)$_2$As$_2$W$_{19}$O$_{67}$(H$_2$O)] (TBA-**1**). TBA-**1** was studied by cyclic voltammetry in acetonitrile (MeCN) solutions containing 0.1 M LiClO$_4$ and compared with the results obtained with Cs-**1** in aqueous media. In MeCN, the Ti^{IV} and W^{VI} waves could not be separated distinctly. An important adsorption phenomenon on the glassy carbon working electrode was encountered both in

cyclic voltammetry and in controlled potential electrolysis and was confirmed by Electrochemical Quartz Crystal Microbalance (EQCM) studies on a carbon film. TBA-**1**, dissolved in MeCN, reacts with H$_2$O$_2$ to give peroxo complexes stable enough for characterization by UV-visible spectroscopy, cyclic voltammetry, and EQCM. TBA-**1** shows high catalytic activity (TOF = 11.3 h^{-1}) in cyclohexene oxidation with aqueous H$_2$O$_2$ producing products typical of a heterolytic oxidation mechanism. The stability of TBA-**1** under turnover conditions was confirmed by using IR, UV-visible spectroscopy as well as cyclic voltammetry.

Keywords: electrochemistry · homogeneous catalysis · polyoxometalates · self-assembly · titanium · tungsten

[a] Dr. F. Hussain, B. S. Bassil, Prof. U. Kortz⁺
International University Bremen, School of Engineering and Science
P.O. Box 750561, 28725 Bremen (Germany)
Fax: (+49)421-200-3229
E-mail: u.kortz@iu-bremen.de

[b] Prof. O. A. Kholdeeva, Dr. M. N. Timofeeva
Boreskov Institute of Catalysis, Russian Academy of Sciences
Lavrentiev avenue 5, Novosibirsk 630090 (Russia)
Fax: (+7)383-330-95-73
E-mail: khold@catalysis.nsk.su

[c] Dr. P. de Oliveira, Dr. B. Keita, Prof. L. Nadjo
Laboratoire de Chimie Physique, UMR 8000, CNRS
Equipe d'Electrochimie et Photoélectrochimie Université Paris-Sud,
Bâtiment 350
91405 Orsay Cedex (France)
Fax: (+33)1-69-15-43-28
E-mail: nadjo@lcp.u-psud.fr

[d] Dr. F. Hussain
School of Chemistry
University of Melbourne
Parkville, Victoria 3010 (Australia)

[⁺] International University Bremen renamed to Jacobs University Bremen as of Spring 2007

Supporting information for this article is available on the WWW under http://www.chemeurj.org/ or from the author: a) Thermogram and heat flow of Cs-**1** and TBA-**1** from RT to 900 and 800°C, respectively; b) UV/Vis spectra of TBA-**1** and TBA-As$_2$W$_{19}$ in the absence and presence of H$_2$O$_2$; c) evolution of the cyclic voltammograms of TBA-**1** as a function of reversal potential; d) cyclic voltammogram of TBA-As$_2$W$_{19}$; e) comparison of the cyclic voltammograms of TBA-**1** and TBA-As$_2$W$_{19}$ in the presence of H$_2$O$_2$.

Introduction

Polyoxometalates (POMs) are an important class of inorganic compounds and they exhibit a diverse compositional range and significant structural versatility. POMs are usually composed of early transition-metal MO_6 (M: W^{6+}, Mo^{6+}, V^{5+}, Nb^{5+}, Ta^{5+}) octahedra and main-group XO_4 (X: P, Si, and so on) tetrahedra.[1] The most famous POMs are probably the Keggin (e.g., $[PW_{12}O_{40}]^{3-}$) and the Wells–Dawson (e.g., $[P_2W_{18}O_{62}]^{6-}$) ions. Although tungstophosphates represent the largest subclass of POMs, many other elements besides phosphorus can act as heteroatoms, for example, As, Si, Ge, B. Interestingly, also elements containing lone pairs, such as, As^{III}, Se^{IV}, can act as heterogroups. The growing interest in POMs undoubtedly reflects their discrete, molecular nature combined with highly flexible and tunable molecular composition, size, shape, charge density, redox potentials, acidity, and solubility characteristics and high thermal stability. As a result, POMs can be used over a wide range of applications including homogeneous and heterogeneous oxidation catalysis, acid/electro-/photocatalysis, biomedicine, materials science, data storage, sensors, and nano/biotechnology.[2] Although POMs have been known for almost 200 years, their mechanism of formation and their structure/composition–activity relationship is not yet fully understood. Therefore, the rational synthesis of new structural types of POMs remains an important research objective.

Titanium-containing POMs are of interest for fundamental structural aspects and also for their associated properties which can lead to interesting applications in catalysis and medicine.[3] Yet, these compounds can be successfully used as tractable soluble probes of heterogeneous single-site titanium catalysts.[4] It is well known that substitution of tungsten(VI) addenda sites by titanium(IV) in a fully oxidized polyoxotungstate increases the basicity of the POM. As a result, almost all known titanium-containing POMs exhibit a strong tendency towards dimer formation through Ti−O−Ti bonds in aqueous solution. Furthermore, most Ti-POMs are based on the Keggin structure as a basic building block.

Some of us have also been interested in Ti-substituted POMs for some time. We reported that interaction of titanium(IV) with the trilacunary Wells–Dawson derivative $[P_2W_{15}O_{56}]^{12-}$ in aqueous acidic solution can lead to a variety of products, including unexpected dimeric and tetrameric structures.[3d] Then we showed that the dilacunary decatungstosilicate $[\gamma\text{-}SiW_{10}O_{36}]^{8-}$ reacts with titanium(IV) to form an unprecedented tetrameric, cyclic assembly.[3e]

In spite of the number of Ti^{IV}-substituted POMs published to date, electrochemical techniques were only occasionally used to complete their characterisations. Among recent achievements, experiments carried out with mercury working electrodes in acetate buffer[5,6] and on glassy-carbon working electrodes in aqueous solutions,[7,8] or in acetonitrile,[3a,9] are illustrative of the main behavior of these complexes. In aqueous solutions with mercury electrodes, the Ti^{IV} center is reduced to the Ti^{III} state and the corresponding process is usually found at a less-negative potential than the onset re-

duction potential of W^{VI} centers.[5,6] The same situation seems to prevail when a glassy-carbon working electrode was used in aqueous media[7,8] even though the clear assignment of the Ti^{IV} to Ti^{III} wave was not always shown. In acetonitrile solution, the focus was directed on the influence of protonation on the cyclic voltammogram waves run on a glassy carbon electrode.[3a,9] On the other hand, the literature on organotitanium[10] compounds would suggest the assignment of the first voltammetric wave system to the one-electron redox couple of the titanium center.

Here, we report on the synthesis, structure, electrochemistry, and oxidation catalysis of the dititanium-containing 19-tungstodiarsenate(III) $[Ti_2(OH)_2As_2W_{19}O_{67}(H_2O)]^{8-}$ (**1**).

Results and Discussion

Synthesis and structure: The dititanium containing 19-tungstodiarsenate(III) $[Ti_2(OH)_2As_2W_{19}O_{67}(H_2O)]^{8-}$ (**1**) has been synthesized in aqueous, acidic medium (pH 2). This novel POM was structurally characterized in the solid state in the form of a hydrated cesium salt, Cs_8-$[Ti_2(OH)_2As_2W_{19}O_{67}(H_2O)]\cdot2\,CsCl\cdot12\,H_2O$ (Cs-**1**). Polyanion **1** comprises two ($B\text{-}\alpha\text{-}As^{III}W_9O_{33}$) Keggin moieties linked through an octahedral $\{WO_5(H_2O)\}$ fragment and two unprecedented square-pyramidal $\{TiO_4(OH)\}$ groups, leading to a sandwich-type structure with nominal C_{2v} symmetry (see Figure 1).
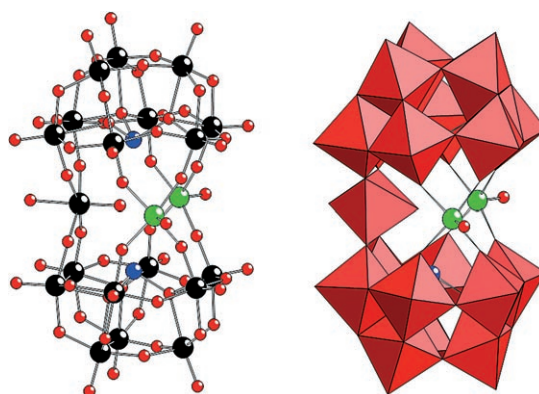

Figure 1. Ball-and-stick (left) and polyhedral (right) representation of $[Ti_2(OH)_2As_2W_{19}O_{67}(H_2O)]^{8-}$ (**1**). The balls are tungsten (black), oxygen (red), titanium (green), arsenic (blue) and the red polyhedra represent WO_6.

Alternatively, **1** can be described as a dilacunary $[As_2W_{19}O_{67}(H_2O)]^{14-}$ fragment which has taken up two Ti^{IV} centers. Some time ago we determined the solid-state structure of $[As_2W_{19}O_{67}(H_2O)]^{14-}$ and also that of a mono-Ni^{II}-containing derivative.[11] The title polyanion **1** closely resembles $[M_2(OH_2)_2As_2W_{19}O_{67}(H_2O)]^{10-}$ (M: Mn^{II}, Co^{II}, Zn^{II}) which we reported a few years ago.[12] In these derivatives the two transition metals and one tungsten atom were statistically disordered over all three belt positions. Therefore, it

could not be concluded with certainty if the aqua ligand of the unique tungsten center points inside or outside of the central cavity. Furthermore, the terminal aqua ligands of the 3d transition-metal centers were disordered with the external ligand of the unique tungsten center. On the other hand, there is no such disorder in **1** at all. Based on bond-valence-sum (BVS)[13] calculations we confirmed that the oxo ligand O11T ($d_{W11-O11T} = 1.77(3)$ Å, $s = 1.60$) of the central tungsten center W11 points inside the polyanion, and the *trans*-related aqua ligand O11A ($d_{W11-O11A} = 2.14(3)$ Å, $s = 0.55$) points outside (see Figure 2). We believe that the same bonding sit-
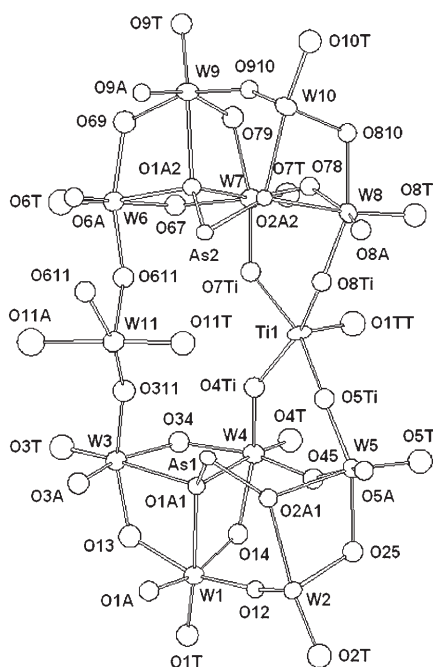

Figure 2. Ball and stick representation of the asymmetric unit of $[Ti_2(OH)_2As_2W_{19}O_{67}(H_2O)]^{8-}$ (**1**) showing 50% probability ellipsoids and the labeling scheme.

uation applies to the unique tungsten center in the above-mentioned $[M_2(OH_2)_2As_2W_{19}O_{67}(H_2O)]^{10-}$ (M: Mn^{II}, Co^{II}, Zn^{II}). Interestingly, the unique tungsten center in the dilacunary precursor $[As_2W_{19}O_{67}(H_2O)]^{14-}$ also exhibits an external aqua and an internal oxo ligand.[11]

The two structurally equivalent titanium atoms in **1** are five-coordinated and exhibit a square-pyramidal coordination geometry (see Figures 1 and 2). As a result, the titanium atoms are situated well above the plane of the four equatorial μ_2-oxo ligands being displaced towards the terminal ligand. This resembles the coordination environment of the organotin centers in our $[Na(H_2O)-(C_6H_5Sn)_2As^{III}_2W_{19}O_{67}(H_2O)]^{7-}$, which was prepared by reaction of $(C_6H_5)SnCl_3$ with $[As_2W_{19}O_{67}(H_2O)]^{14-}$ in aqueous medium at pH 1.6.[14] The square-pyramidally coordinated tin atoms are significantly displaced towards the terminal aryl groups. Also in this polyanion the unique tungsten center exhibits an external aqua and an internal oxo ligand.

The fact that **1** contains titanium centers with terminal ligands is a rather exciting aspect, as most structurally characterized Ti^{IV}-containing POMs exhibit Ti−O−Ti bridges.[3] Now the question arises on the exact nature of the terminal ligands of Ti in **1**. For di- or trivalent 3d transition-metal centers the terminal ligands are usually diprotonated oxygen atoms, that is, water. However, in the case of the early, tetravalent transition-metal titanium this is much less likely. Therefore, we performed BVS calculations on **1** for the oxygens in question. The BVS value of $s = 1.4$ strongly suggests that O1TT and O1TT′ are each monoprotonated, which means that the ligands are not H_2O but rather OH^- (see Figure 2). This is fully consistent with the observation that POMs containing Ti^{IV} exhibit a strong tendency in aqueous solution for intermolecular Ti−O−Ti bond formation resulting in the linkage of two or more POM fragments through the following condensation step:[3]

$$POM\text{-}Ti\text{-}OH + HO\text{-}Ti\text{-}POM' \rightarrow POM\text{-}Ti\text{-}O\text{-}Ti\text{-}POM' + H_2O$$
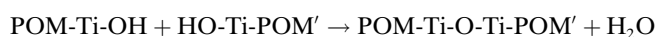
The relative orientation of the two titanium centers in **1** does not allow for intramolecular Ti−O−Ti bond formation. Furthermore, dimer formation by linkage of two units of **1** through intermolecular Ti−O−Ti′ bonds is also not very likely due to steric reasons. It can be noticed that the terminal hydroxo ligands of the two titanium centers are not very exposed and therefore hardly accessible for hydroxo ligands of neighboring polyanions. The terminal oxo groups (O4T, O5T, O7T, O8T) of the four adjacent tungsten centers (W4, W5, W7, W8) exhibit a steric shielding effect. This appears to be the main reason why the terminal hydroxo ligands in **1** prevail in aqueous solution.

Polyanion **1** was synthesized in a one-pot reaction by interaction of titanium(IV)-oxosulfate {$TiOSO_4$} with $K_{14}[As_2W_{19}O_{67}(H_2O)]$ in aqueous, acidic medium (pH 2). However, we obtained **1** for the first time accidentally during a reaction of $TiOSO_4$ with $Na_9[\alpha\text{-}AsW_9O_{33}]$ in a molar ratio of 4:1 in aqueous medium at pH 4. Then we decided to reproduce **1** via a more rational synthetic procedure by using the dilacunary precursor $[As_2W_{19}O_{67}(H_2O)]^{14-}$ (see Experimental Section). The 19-tungstodiarsenate(III) $[As_2W_{19}O_{67}(H_2O)]^{14-}$ was synthesized for the first time about 30 years ago by Tourné et al. and recently, Kortz et al. confirmed the proposed structure by X-ray diffraction.[11,15] Interestingly, to date only a few polyoxoanions have been synthesized by using $[As_2W_{19}O_{67}(H_2O)]^{14-}$ as a precursor.[11,16]

The equatorial Ti−O bond lengths in **1** are rather regular, ranging from 1.963–1.985(16) Å. The O-Ti-O1TT angles (98.7–102.0(8)°) reflect the displacement of the Ti centers towards the terminal hydroxo ligand O1TT. The metal–metal and As–As distances in the central belt of **1** are as follows: Ti1···Ti1′ 5.09 Å, Ti1/Ti1′···W11 4.60 Å, As1···As2 5.49 Å.

In addition to the terminal aqua ligand (W−OH_2) and the two terminal hydroxo ligands (Ti−OH) there are no other

protonation sites in **1**. As a result, the charge of polyanion **1** is −8. Interestingly, this charge is balanced exclusively by cesium ions which completely surround **1**. Furthermore, two equivalents of cesium chloride cocrystallized with Cs-**1** as based on XRD and elemental analysis. The TBA salt of **1** was prepared by addition of solid TBABr to a freshly synthesized solution of **1**, isolated by suction filtration, washed with plenty of water, and then dried in an oven at 50 °C overnight. Purity of TBA-**1** was confirmed by IR, elemental analysis, TGA, and electrochemistry.

UV-visible spectrophotometry: TBA-**1** and the corresponding lacunary precursor (TBA)$_7$H$_7$[As$_2$W$_{19}$O$_{67}$(H$_2$O)] (TBA-As$_2$W$_{19}$) were studied by both UV-visible spectrophotometry and electrochemistry. As expected, the presence of titanium atoms in the POM structure gives rise to a markedly different behavior.

Both species TBA-**1** and TBA-As$_2$W$_{19}$ are soluble in acetonitrile, and TBA-**1** is stable over several hours, but the spectrum of the lacunary precursor starts changing about one hour after the solution has been prepared. In addition, TBA-**1** reacts with H$_2$O$_2$, giving rise to a yellow solution exhibiting a UV/Vis absorption band at 400 nm, (see Supporting Information, Figure SI2). It is worth noting that this yellow color is characteristic of the Ti^{IV}-peroxo complex classically used for the detection of hydrogen peroxide in solution.[17] For $\gamma = 10$ (γ is defined as the molar ratio of H$_2$O$_2$ to that of the relevant POM given by: $\gamma = c_{H_2O_2}/c_{POM}$), the 400 nm band slowly evolves with time, increasing by 7% in the first hour and by 15% after 3 h. No significant changes were seen afterwards. This behavior suggests the existence of an induction period. The lacunary precursor salt TBA-As$_2$W$_{19}$ did not react with H$_2$O$_2$ analogously to TBA-**1**: no yellow color was formed, and no new band was detected in the UV-visible spectrum. Analogous experiments were performed on Cs-**1** in aqueous media in the absence of H$_2$O$_2$ and they indicate that **1** is stable in the pH 2–5 media used in this work.

Electrochemistry

Behavior in MeCN and in aqueous media: In Figure 3, the CV of TBA-**1** is restricted to the first redox couple ($E_{pc1} = -0.740$ and $E_{pa1} = -0.520$ V, the former preceded by a pre-wave at -0.694 V and the latter by a pre-wave at $E_{pa} = -0.600$ V). In anticipation of the forthcoming series of experiments with hydrogen peroxide, a voltammetric trace superimposed on Figure 3 shows that no cathodic activity was observed in the potential domain explored, when H$_2$O$_2$ was added to the pure electrolyte. The sharp oxidation process shown in Figure 3 shows the characteristic shape usually encountered for the oxidation of adsorbed species. Upon reversing the scan direction at less and less negative potentials, the progressive onset of the adsorption could be qualitatively observed (Supporting Information, Figure SI3). The corresponding cyclic voltammogram for TBA-As$_2$W$_{19}$ is constitut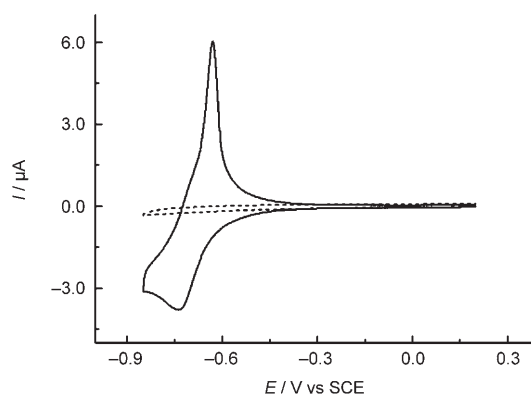ed by a rather drawn-out pre-wave around -0.500 V followed by a reduction wave at -0.850 V. Upon scan direction reversal, no sharp oxidation peaks were observed, in contrast to the case of TBA-**1**. The voltammetric characteristics are clearly different for the two polyanion salts TBA-**1** and TBA-As$_2$W$_{19}$, differences which are likely due to the presence of titanium(IV) in the former.

Figure 3. Comparison of the cyclic voltammograms of 2×10^{-4} M TBA-**1** in acetonitrile (——) and 4×10^{-4} M H$_2$O$_2$ in 0.1 M LiClO$_4$ solution in acetonitrile (-----), respectively. The scan rate was 10 mV s^{-1}. The working electrode was a glassy carbon disk and the reference electrode was a saturated calomel electrode (SCE). For further details, see text.

Controlled potential electrolysis of 2×10^{-4} M TBA-**1** was performed in 0.1 M LiClO$_4$ in MeCN. At -0.580 V (i.e., within the potential domain of the reduction pre-wave), the electrolysis gave rise to a blue-colored solution, an indication that W atoms were being reduced. Then, the potential was stepped to -0.760 V (i.e., beyond the reduction peak maximum) for further electrolysis and as a result the blue color of the solution intensified. During this electrolysis, a significant amount of material deposited on the working electrode surface. The development of a blue color, whatever the potential selected for the electrolysis, indicated unambiguously the mixing of Ti and W waves. The process turned out to be irreversible, and an attempt to reoxidize the reduced species at $+0.2$ V resulted in consumption of less than one tenth of the charge passed upon reduction. In fact, the final voltammogram was somewhat different from the first one, the oxidation wave being shorter and broader.

The cyclic voltammetry behavior of Cs-**1** in aqueous media was useful to shed more light on the observations made in MeCN. For example, in the pH 3 medium, the CV pattern of Cs-**1** is featured two closely spaced, drawn out reduction peaks followed by a large-current composite wave. The first two waves are associated with small, but distinctly separated oxidation waves on potential reversal ($E_{pc1} = -0.600$ V and $E_{pa1} = -0.356$ V and $E_{pc2} = -0.710$ V and $E_{pa2} = -0.528$ V, respectively). This is similar to the behavior exhibited by the potassium salt of the dititanium-containing decatungstophosphate, K$_7$[Ti$_2$W$_{10}$PO$_{40}$]·6H$_2$O, in 1 M H$_2$SO$_4$.[8] These waves are pH-dependent and the overall voltammetric pattern remains unchanged in the pH 2–5 domain studied in this work, with the following trends: i) the waves are better separated with increasing pH; ii) in

contrast, for a given pH, the waves tend to mix as the scan rate increases; iii) whatever the scan rate, no tendency towards strong adsorption was observed throughout the pH domain studied.

Controlled potential coulometry of Cs-**1** was carried out in the pH 3 medium at two selected potential values. At $E = -0.600$ V, no blue color was visible in the solution even after complete consumption of the charge necessary for a one-electron process. Importantly, all the consumed charge could be recovered upon reoxidation of the solution. In contrast, a faint blue color was observed when the potential was set at $E = -0.750$ V. It is worth noting that no deep blue color developed even after the consumption of roughly five electrons per molecule of **1**, a feature that might be rationalized by polyanion-catalyzed solvent reduction. A faint blue color appeared when a controlled potential electrolysis was carried out at $E = -0.510$ V at pH 2. In short, CV and controlled potential electrolysis experiments of Cs-**1** in aqueous media are consistent and confirm why no irreversible deposit occurs on the working electrode surface. In addition, the separation of the Ti and W waves depends critically on the pH of the electrolyte.

Altogether, these experiments in aqueous media provide results which are complementary to those obtained in MeCN, thereby shedding light on the latter. The results with Cs-**1** in aqueous media support the conclusion that the first reduction wave of TBA-**1** in MeCN must be associated with the redox processes of both the Ti and W centers.

Influence of H$_2$O$_2$: The main results of the role of H$_2$O$_2$ are illustrated in Figure 4. The cyclic voltammograms observed in the absence and then in the presence of increasing quantities of H$_2$O$_2$ are superimposed. The voltammetric pattern associated with TBA-**1** evolved markedly upon addition of increasing amounts of H$_2$O$_2$. We used the same potential domain as previously in the absence of H$_2$O$_2$. Table 1 shows the main characteristics of the cyclic voltammograms shown in Figure 4.
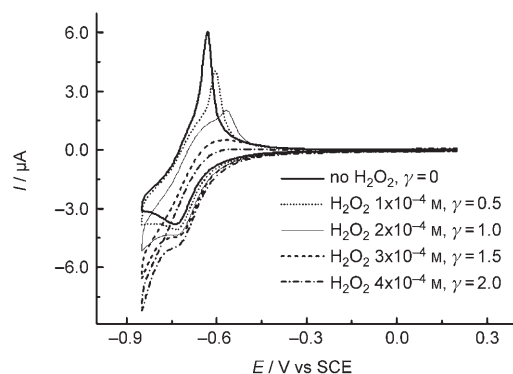

Figure 4. Evolution of the cyclic voltammogram of 2×10^{-4} M TBA-**1** in 0.1 M LiClO$_4$ solution in acetonitrile as a function of the concentration of H$_2$O$_2$ (or as a function of γ). The scan rate was 10 mV s^{-1}. The working electrode was a glassy carbon disk and the reference electrode was a saturated calomel electrode (SCE). For further details, see text.

Table 1. Main characteristics of the cyclic voltammograms of TBA-**1** presented in Figure 4. For further details, see text.

γ	E_c [V]	I_c [μA]	E_a [V]	I_a [μA]	E_a (pre-wave) [V]	I_a (pre-wave) [μA]
0	−0.738	−3.80	−0.630	6.04	−0.694	1.11
0.5	−0.731	−4.07	−0.605	4.05	−0.670	1.29
1.0	−0.734	−4.37	−0.568	2.02	−0.630	1.31
1.5	−0.728	−4.42	−0.579	0.50	(−0.579)	0.50
2.0	−0.732	−4.94	not seen			

Some general trends become apparent: i) the cathodic wave does not change its position but the overall current intensity increases slightly with the excess parameter γ; ii) upon potential reversal, the composite oxidation pattern observed previously remains composite up to $\gamma = 1.5$, but with largely decreased current intensities; in addition, a positive potential shift of the adsorption wave results in a better separation of the waves. For $\gamma = 2$, chemical irreversibility is observed, with complete disappearance of the adsorption phenomenon; iii) strikingly, what seems to be a new cathodic wave following the initial one appears and increases with increasing γ values. It is worth emphasizing again that no direct reduction of H$_2$O$_2$ was observed in this potential domain (Figure 3). The corresponding experiments with TBA-As$_2$W$_{19}$ are shown in the Supporting Information (Figures SI4 and SI5), and confirm the difference in behavior compared with that of TBA-**1**.

EQCM characterization: Electrochemical Quartz Crystal Microbalance (EQCM) studies revealed that a product accumulated on the electrode surface upon reduction when the applied potential was more negative than −0.65 V. We noticed that the amount of adsorbed material, which was proportional to the variation of the vibration frequency ΔF, depends on the reverse potential, E_{rev}, (Figure 5a). The mass of the material deposited on the electrode surface kept increasing, even after the scan direction was reversed. A maximum ΔF was obtained at −0.700 V, and upon oxidation the product was removed from the electrode surface. At the final applied potential of +0.200 V the crystal practically returned to its initial vibrating frequency. Therefore, it seems that the deposition process is reversible.

In the presence of H$_2$O$_2$ the behavior was rather different: when the maximum ΔF was reached, it decreased no more than a few percent when reaching the initial potential of +0.2 V, meaning that the process is irreversible in the potential range considered (Figure 5b). Nevertheless, the crystal frequency recovered substantially upon subsequent scanning from +0.200 up to +1.000 V.

At the very least, this series of EQCM experiments confirms the formation of an adduct between TBA-**1** and H$_2$O$_2$, with an electrochemical deposition behavior substantially different from that of TBA-**1** alone.

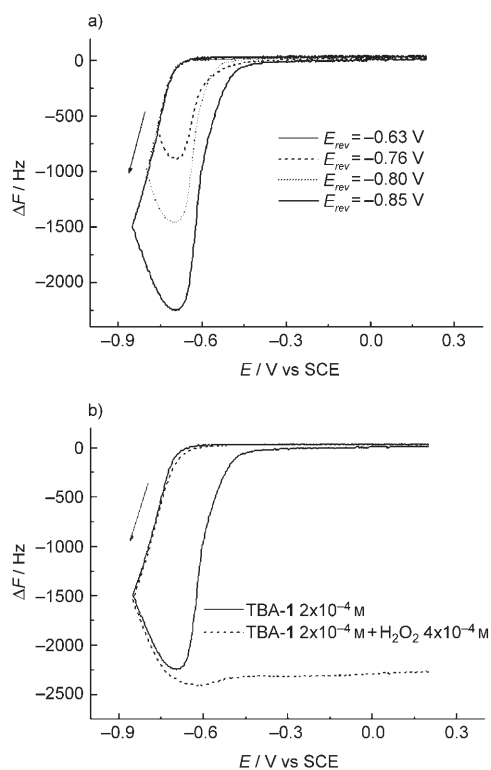**Catalytic oxidation of cyclohexene (CyH)**: The results on CyH oxidation with aqueous hydrogen peroxide catalyzed

Figure 5. a) Evolution of ΔF as a function of the potential reversal as obtained by QCM for 2×10^{-4} M TBA-**1** in 0.1 M LiClO$_4$ solution in acetonitrile. b) Comparison of the variation of ΔF as obtained by QCM for 2×10^{-4} M TBA-**1** in 0.1 M LiClO$_4$ solution in acetonitrile in the absence and presence of 4×10^{-4} M H$_2$O$_2$. The scan rate was 10 mV s^{-1}; the working electrode was a glassy carbon disk and the reference electrode was a saturated calomel electrode (SCE). For further details, see Figure 4.

by the three Ti-containing polytungstate salts TBA-**1**, $[Bu_4N]_7[(PTiW_{11}O_{39})_2OH]$ (TBA-**2**),[3a,j] and $[Bu_4N]_{12}H_{12}[\beta\text{-}Ti_2SiW_{10}O_{39}]_4$ (TBA-**3**),[3e] as well as the data published previously for NaH$_4$PW$_{11}$TiO$_{40}$[3i] are given in Table 2. The catalytic activity of the polyanions, normalized to the amount of Ti (TOF$_{Ti}$), decreased in the order $\mathbf{1} \gg \mathbf{2} > \mathbf{3}$. In the presence

of both **2** and **3**, the CyH oxidation produced the allylic oxidation products, 2-cyclohexen-1-ol and 2-cyclohexen-1-one, along with comparable amounts of the corresponding epoxide and diol (Scheme 1).
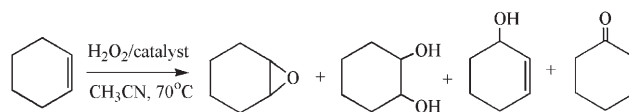
Scheme 1.

Such a product distribution is characteristic for a homolytic oxidation mechanism[18] and is typical for POMs containing Ti−OH groups isolated in an inorganic matrix, which are capable of forming a monoprotonated peroxo-titanium complex.[3j,4,9]

In sharp contrast, polyanion **1** affords epoxide, diol, and products of the diol overoxidation but none of the allylic oxidation products (Scheme 2).

This indicates a heterolytic oxidation mechanism through oxygen transfer from an active peroxo species to the alkene.[18,19] As one can judge from the data presented in Table 2 (TOF$_{Ti}$) and Figure 6, the catalytic activity of **1** was significantly higher than that of **2** and **3**. At the same time, the activity of **1**, normalized to equivalents of W (TOF$_W$), was lower by just a factor of 3–4 compared with the activity of the well-known Venturello polyanion $\{PO_4[W(O)(O_2)_2]_4\}^{3-}$. However, while the Venturello complex, in accordance with the literature,[19,20] gave a high yield of epoxide, *trans*-cycloxehane-1,2-diol predominated amongst the oxidation products obtained in the presence of TBA-**1**. A similar catalytic behavior was found recently for the Ti-monosubstituted Keggin POMs Na$_{5-n}$H$_n$PTiW$_{11}$O$_{40}$ with $n = 2–5$ (see Table 2).[3i] Based on the results obtained in that work, the authors hypothesized on the necessity for two protons in the transition state to activate the peroxo group for an oxygen-transfer mechanism.[3i,4] It is worth

Table 2. Cyclohexene oxidation with H$_2$O$_2$ catalysed by various Ti-POMs.[a]

POM	Concentration [mM]			CyH conv [% mol]	Selectivity[b] [% mol]					TOF$_{Ti}$[c] [h^{-1}]	TOF$_W$[d] [h^{-1}]
	[POM]	[Ti]	[W]		(epoxide)	(en-ol)	(en-one)	(diol)	Other		
TBA-**1**	3.8	7.6	72.2	100	11	trace	trace	49	40[e]	11.3	1.2
				100[f]	13[f]	trace	trace	51[f]	36[f]		
TBA-**2**	3.9	7.8	85.8	45	28	23	16	29	4	2.1	0.2
TBA-**3**	1.3	10.4	52.0	31	29	15	38	12	6	1.2	0.2
Cet$_3$PW$_4$O$_{24}$	1.3	–	5.2	35	77	2	trace	15	6	–	3.6
Aliq$_3$PW$_4$O$_{24}$	1.3	–	5.2	52	82	2	trace	12	4	–	4.6
NaH$_4$PW$_{11}$TiO$_{40}$[3i]	10.0	10.0	110	84	7	2	5	75	11	n.d.[f]	n.d.

[a] Reaction conditions: CyH (0.6 mmol), H$_2$O$_2$ (1.2 mmol), CH$_3$CN (3 mL), 70°C, 4 h. [b] GC yield based on CyH consumed. [c] TOF$_{Ti}$ = (moles of CyH consumed)/(moles of Ti × time); determined from the initial rates of CyH consumption. [d] TOF$_W$ = (moles of CyH consumed)/(moles of W × time); determined from the initial rates of CyH consumption. [e] Mainly products of the diol overoxidation: cyclohexanol-2-one (≈ 65%), cyclooxoheptane-ol-1-one-6 and adipic acid anhydride. [f] The catalyst was used repeatedly. [g] Not determined.
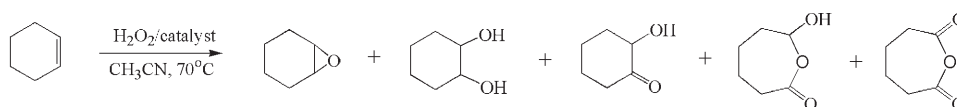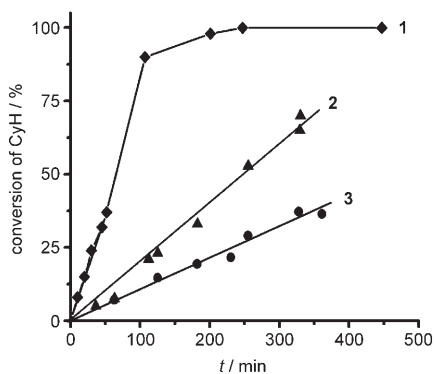
Scheme 2.

Figure 6. CyH oxidation with H_2O_2 in CH_3CN (CyH, 0.2 M; H_2O_2, 0.4 M; 70°C) catalyzed by tetra-n-butyl ammonium salts of $[Ti_2(OH)_2As_2W_{19}O_{67}(H_2O)]^{8-}$ (**1**, 3.8 mM), $[(PTiW_{11}O_{39})_2OH]^{7-}$ (**2**, 3.9 mM), and $[\{\beta\text{-}Ti_2SiW_{10}O_{39}\}_4]^{24-}$ (**3**, 1.3 mM).
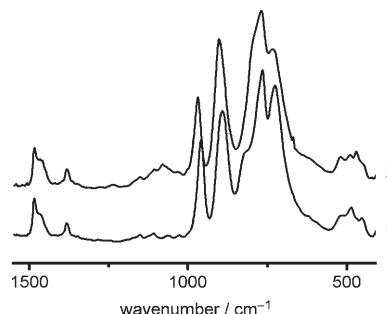

Figure 7. IR spectra of TBA-**1** before (1) and after (2) the reaction of CyH oxidation. Reaction conditions as in Table 2; after the reaction, the catalyst was precipitated by addition of water, separated by centrifugation, washed with water, and dried in vacuum at 50°C for 3 h.

noting that the structure of polyanion **1**, in which two Ti– OH groups (and a $WO(H_2O)$ fragment) are present close to each other, completely satisfies this requirement. Therefore, the high catalytic activity of **1** in the heterolytic CyH oxidation with H_2O_2 supports the above-mentioned hypothesis.

Several ^{31}P NMR studies have indicated that many POMs are not stable in solution towards H_2O_2. In fact, these POMs often act as precursors for the true catalyst, for example the Venturello complex and/or other low nuclearity peroxotungstates.[19,21–23] The resistance towards H_2O_2 is known to increase with increasing POM charge.[19] To ascertain correct interpretation of the catalytic results, we addressed the question of stability of **1** in the presence of an excess of H_2O_2. The absence of P as a heteroatom in the structure of **1** did not allow us to perform the stability study by using ^{31}P NMR as done previously for several Ti-monosubstituted POMs.[3a,j,4] However, the stability of **1** under turnover conditions was confirmed by IR and UV-visible spectroscopy as well as cyclic voltammetry (see above).

As mentioned above, the TOF_W value determined for **1** is 3–4 times lower than that of the Venturello complex (see Table 2). Therefore, one might expect that about 25–33% of **1** would be converted to low nuclearity species, if the catalytic activity were due to tungsten-peroxo species rather than titanium-peroxo species. Figure 7 shows the IR spectra of TBA-**1** before and after the oxidation of CyH with H_2O_2. We could not observe significant changes in the spectrum collected after the reaction, indicating that no transformation of **1** to a Venturello-like species had occurred. It is important to note that the catalyst TBA-**1** can be used repeatedly. The catalytic performance of TBA-**1** that had been separated after the reaction, washed, dried, and then added to

a fresh reaction mixture, was nearly the same as in the first catalytic cycle (Table 2).

After addition of a 100-fold excess of H_2O_2 to TBA-**1** dissolved in MeCN, a strong absorption (shoulder) located at 393–400 nm gradually appeared in the UV-visible spectrum. According to the literature,[9,24,25] this band can be attributed to the $O_2 \rightarrow Ti$ ligand-to-metal charge-transfer band. Importantly, the intensity of this band does not decrease while keeping the solution at 70°C for several days. As tungstenperoxo POMs are expected to be colorless, the formation of a yellow peroxo-titanium-POM species upon interaction with H_2O_2 is one more argument in favor of the stability of **1**, with respect to solvolytic destruction in the presence of hydrogen peroxide. These conclusions are also supported by our electrochemistry results (see above). We also performed ^{183}W NMR experiments on TBA-**1** in MeCN and on Cs-**1** in water, but in both cases the signal-to-noise ratio of the spectra was poor due to low solubility and did not allow us to draw definitive conclusions.

In any case, our combined experimental data allow us to suggest that a protonated titanium-peroxo derivative of **1** is the active intermediate responsible for the high catalytic activity of this polyanion in the oxygen-atom transfer from H_2O_2 to alkene. Attempts to isolate this peroxo-POM species and to study its structure and reactivity under stoichiometric conditions are in progress in our groups.

Conclusion

We have synthesized the dititanium-containing 19-tungstodiarsenate(III) $[Ti_2(OH)_2As_2W_{19}O_{67}(H_2O)]^{8-}$ (**1**) in aqueous, acidic medium (pH 2) by a one-pot reaction of $TiOSO_4$ with the dilacunary POM precursor $[As_2W_{19}O_{67}$

$(H_2O)]^{14-}$. We isolated **1** as a cesium salt, as well as, a TBA salt, which allowed us to perform solution studies in aqueous and organic media. Polyanion **1** was characterized in the solid state by a variety of analytical techniques including single-crystal XRD, IR, elemental analysis, and TGA. Polyanion **1** represents a new member of the small class of titanium-containing polytungstates. Incorporation of two neighbouring Ti^{IV} centers with a terminal hydroxo ligand each represents probably the most important and also unique structural feature of **1**. The unprecedented arrangement of the two reactive TiOH groups in **1** allows neither for intra- nor intermolecular Ti−O−Ti bond formation. As a result, the (TiOH)$_2$ active site within **1** is well protected and thus available for interaction with small molecules or ions. Polyanion **1** is surprisingly stable in aqueous and organic solvents, which allowed us to perform a variety of electrochemical and catalytic studies. In particular, we investigated the reactivity of TBA-**1** with cyclohexene in the presence of hydrogen peroxide in order to evaluate the potential of our POM as a homogeneous oxidation catalyst.

UV-visible, cyclic voltammetry, and EQCM experiments were used to evaluate the stability and redox behavior of TBA-**1** and its lacunary precursor, TBA-As$_2$W$_{19}$, in MeCN solutions, under various conditions. TBA-**1** is stable for much longer than TBA-As$_2$W$_{19}$. There is a marked difference between their cyclic voltammetry responses as a consequence of Ti substitution in TBA-**1**. The Ti^{IV} and W^{VI} waves of TBA-**1** could not be separated distinctly in MeCN. EQCM studies on a carbon film confirmed the adsorption phenomenon also observed in both cyclic voltammetry and controlled-potential electrolysis. In contrast, our studies with Cs-**1** in aqueous pH 3 buffer allowed to clearly assign the first reduction wave to a redox process involving the Ti^{IV} centers. Furthermore, no irreversible deposition process was observed in these media. We found that the lacunary precursor TBA-As$_2$W$_{19}$ did not react with H$_2$O$_2$ to any appreciable extent in MeCN, independent of the experimental parameters. In contrast, TBA-**1** reacts with H$_2$O$_2$ to give derivatives which could be characterized by UV-visible spectroscopy, cyclic voltammetry, and EQCM and which were found to be stable over the timescale of several hours. These features designate TBA-**1** as a candidate for oxidation processes in the presence of H$_2$O$_2$.

Indeed, TBA-**1** shows high catalytic activity in H$_2$O$_2$-based cyclohexene oxidation producing mainly epoxide, and *trans*-cycloxehane-1,2-diol, the products typical of a heterolytic oxidation mechanism. The stability of TBA-**1** with respect to solvolytic destruction under turnover conditions was confirmed using IR, UV-visible, and cyclic voltammetry. The unprecedented high activity of **1** in heterolytic cyclohexene oxidation with H$_2$O$_2$ is most likely due to the two Ti−OH groups (or Ti−OH and WO(H$_2$O) fragments), which are close to each other and thus favor the formation of a diprotonated peroxo-titanium POM species capable of oxygen atom transfer to alkenes.

Experimental Section

Synthesis: The precursor K$_{14}$[As$_2$W$_{19}$O$_{67}$(H$_2$O)] was synthesized according to the published procedure of Kortz and et al. and the purity was confirmed by infrared spectroscopy.[11] All other reagents were used as purchased without further purification.

Cs$_8$[Ti$_2$(OH)$_2$As$_2$W$_{19}$O$_{67}$(H$_2$O)]·2CsCl·12H$_2$O (Cs-1): A sample of TiOSO$_4$ (0.14 g, 0.88 mmol) was dissolved in H$_2$O (40 mL) followed by addition of K$_{14}$[As$_2$W$_{19}$O$_{67}$(H$_2$O)] (2.10 g, 0.40 mmol). This solution (pH 2.0) was heated to 80 °C for 1 h, cooled to RT, and filtered. Then CsCl (0.5 mL, 0.1 M) was added and this solution was allowed to evaporate in an open vial at RT. A light-yellow crystalline product started to appear after about 1–2 weeks. Evaporation was continued until the solvent approached the solid product (1.43 g, 55 %). IR: $\tilde{\nu}$ = 963(m), 897(m), 761(s), 723(s), 615(sh), 512(sh), 483(w), 449 cm^{-1} (sh); elemental analysis calcd (%) for Cs-**1**: Cs 20.5, W 53.9, Ti 1.5, As 2.3; found: Cs 20.0, W 52.6, Ti 1.7, As 2.0.

{(n-C$_4$H$_9$)$_4$N}$_5$H$_3$[Ti$_2$(OH)$_2$As$_2$W$_{19}$O$_{67}$(H$_2$O)] (TBA-1): The tetra-*n*-butylammonium (TBA) salt of **1** was prepared by adding an excess of solid TBABr to a freshly synthesized solution of **1**. The resulting white precipitate was isolated by suction filtration, washed with plenty of H$_2$O, and then dried overnight in an oven at 50 °C. Elemental analysis calcd (%) for TBA-**1**: W 57.5, Ti 1.6, As 2.5, N 1.2, C 15.8, H 3.1; found: W 58.6, Ti 1.7, As 2.4, N 1.2, C 15.1, H 3.4. Also thermogravimetric analysis (TGA) fully supports the presence of four TBA cations per formula unit (see Supporting Information, Figure SI2).

The TBA salt of [As$_2$W$_{19}$O$_{67}$(H$_2$O)]$^{14-}$ (TBA-As$_2$W$_{19}$) was prepared by an analogous procedure.

Elemental analyses were performed by Analytische Laboratorien, Industriepark Kaiserau, 51789 Lindlar, Germany. Infrared spectra were recorded by using KBr pellets on a Nicolet Avatar spectrophotometer. Thermogravimetric analysis was carried out on a TA Instruments SDT Q600 thermobalance with a 100 mL min^{-1} flow of nitrogen; the temperature was ramped from 20 to 800 °C at a rate of 5 °C min^{-1}.

X-ray crystallography: A crystal of compound Cs-**1** was mounted on a glass fiber for indexing and intensity data collection at 200 K on a Bruker SMART APEX II CCD single-crystal diffractometer by using Mo$_{K\alpha}$ radiation (λ = 0.71073 Å). Direct methods were used to solve the structure and to locate the heavy atoms (SHELXS97). Then the remaining atoms were found from successive difference maps (SHELXL97). Routine Lorentz and polarisation corrections were applied and an absorption correction was performed by using the SADABS program.[26] The largest peak in the final difference map was 7.1 e Å^{-3} located 0.74 Å from Ti1. The next largest peak was 4.8 e Å^{-3} located 0.71 Å from W10. The deepest hole was −5.4 e Å^{-3} located 0.39 A from W11. We could detect only 8.5 of the 10 Cs$^+$ ions in Cs-**1** crystallographically. This is not surprising as disordered counter cations and/or crystal waters are a common problem in POM crystallography. We have assigned partial occupancy of 0.5 for some Cs and H$_2$O sites in order to model the disorder, which pushes the XRD refinement to its limits. However, we performed elemental analysis which was fully consistent with Cs-**1** (see above). Crystallographic data are summarized in Table 3. Further details of the crystal structure investigation can be obtained from the Fachinformationszentrum Karlsruhe, D-76344 Eggenstein-Leopoldshafen, Germany (fax: (+49)7247-808-666; e-mail: crysdata@fiz-karlsruhe.de) on quoting the depository number CSD-417416.

Electrochemistry: Acetonitrile and lithium perchlorate were purchased from Sigma–Aldrich. These chemicals were used without further purification. For aqueous solutions, pure water was used throughout. It was obtained by passing through a RiOs 8 unit followed by a Millipore-Q Academic purification set. All reagents were of high-purity grade and were used as purchased without further purification. The UV/Vis spectra were recorded on a Perkin–Elmer Lambda 19 spectrophotometer with 1.2 × 10^{-6} M solutions of the relevant polyanion. Matched 1.000 cm-optical-path quartz cuvettes were used. The composition of the various media was as follows: pH 2 and 3, 0.5 M Li$_2$SO$_4$ + H$_2$SO$_4$; pH 5, 1 M CH$_3$COOLi + CH$_3$COOH.

Table 3. Crystal data and structure refinement for Cs$_8$-[Ti$_2$(OH)$_2$As$_2$W$_{19}$O$_{67}$(H$_2$O)]·2CsCl·12H$_2$O (Cs-**1**).

empirical formula	As$_2$Cl$_2$Cs$_{10}$H$_{28}$O$_{82}$Ti$_2$W$_{19}$
F_w [g mol^{-1}]	6479.1
space group (no.)	$P2_1/m$ (11)
a [Å]	12.7764(19)
b [Å]	19.425(3)
c [Å]	18.149(3)
β [°]	110.23(3)
V [Å^3]	4226.3(12)
Z	2
T [°C]	−73
λ [Å]	0.71073
ρ_{calcd} [Mg m^{-3}]	4.87
μ [mm^{-1}]	30.5
R [$I > 2\sigma(I)$][a]	0.081
R_w (all data)[b]	0.196

[a] $R = \Sigma ||F_o| - |F_c||/\Sigma |F_o|$. [b] $R_w = [\Sigma w(F_o^2 - F_c^2)^2/\Sigma w(F_o^2)^2]^{1/2}$.

Electrochemical experiments: The polyanion concentration was 2×10^{-4} M, unless otherwise indicated. The solutions were thoroughly deoxygenated for at least 30 min with pure argon and kept under a positive pressure of this gas during the experiments. The source, mounting, and polishing of the glassy carbon (GC, Tokai, Japan) electrodes has been described.[27] The glassy carbon samples had a diameter of 3 mm. The electrochemical set-up was an EG&G 273A driven by a PC with the M270 software. Potentials are quoted against a saturated calomel electrode (SCE). This reference electrode was dipped in a 0.1 M LiClO$_4$ acetonitrile solution (or alternatively in the appropriate aqueous supporting electrolyte) and separated from the test solution and closed by a medium-porosity glass frit. The counter electrode was a platinum gauze of large surface area. All experiments were performed at RT.

Electrochemical quartz crystal microbalance (EQCM) measurements: The EQCM set-up used in this work was the system QCA 922 (Seiko/EG&G) with 9 MHz AT-cut crystals. New crystals equipped with carbon electrodes were provided by Seiko and allowed working in media where classical gold or platinum electrodes were inappropriate. The true surface area of this carbon electrode was 0.3 cm^2. The data from the QCA 922 set-up were first recorded on the computer and then printed.[28] Frequency variations were recorded as the only necessary data for the discussion in this work. However, the expressions "mass increase" or "mass decrease" will also be used routinely as equivalents to "frequency decrease" or "frequency increase".

Materials for catalysis studies: Acetonitrile, cyclohexene (CyH), cyclohexene oxide, *trans*-cyclohexane-1,2-diol, 2-cyclohexen-1-ol, and 2-cyclohexen-1-one were purchased from Fluka. All the other reactants were of the best available reagent grade and were used without further purification. H$_2$O$_2$ (30 wt% in water) was titrated iodometrically prior to use.

Catalysts: [Bu$_4$N]$_7$[(PTiW$_{11}$O$_{39}$)$_2$OH] (TBA-**2**, ^{31}P NMR in dry MeCN: −12.76 ppm) was synthesized starting from the heteropolyacid H$_5$PW$_{11}$TiO$_{40}$.[3a,j] The Venturello complex with two different cations, Cet$_3$PW$_4$O$_{24}$ and Aliq$_3$PW$_4$O$_{24}$ (^{31}P NMR in CH$_2$Cl$_2$: 3.04 ppm), was prepared by using [C$_5$H$_5$NC$_{16}$H$_{33}$]Cl (CetCl) (98%, Acros) and [CH$_3$(*n*-C$_8$H$_{17}$)$_3$N]Cl (AliqCl) (Lancaster), respectively, as described previously.[20] [Bu$_4$N]$_{12}$H$_{12}$[β-Ti$_2$SiW$_{10}$O$_{39}$]$_4$ (TBA-**3**) was prepared by the same procedure as TBA-**1** (see above).

Catalytic oxidations: The catalytic oxidations of CyH (0.6 mmol) with H$_2$O$_2$ (1.2 mmol) in the presence of Ti-POMs were carried out in temperature-controlled glass vessels at 70°C in MeCN solution (3 mL). Pentadecane was added as the internal standard. Samples were taken during the course of the reaction, and the reaction products were identified by GC-MS (a Saturn 2000 gas chromatograph equipped with a CP-3800 mass spectrometer) and were quantified by GC (gas chromatograph Tsvet-500 equipped with a flame-ionization detector and a 2 m × 3 mm column filled with 5% SE-30/Chromosorb N-AW-DMCS). The TOF (turnover frequencies) values were determined from the initial rates of CyH consumption. After the reaction, water was added to the reaction mixture and the catalyst TBA-**1** was separated by centrifugation, washed with water, dried at 50°C in vacuum, and reused.

[1] a) M. T. Pope, *Heteropoly and Isopoly Oxometalates*, Springer, Berlin, **1983**; b) M. T. Pope, A. Müller, *Angew. Chem.* **1991**, *103*, 56–70; *Angew. Chem. Int. Ed. Engl.* **1991**, *30*, 34–48.

[2] a) *Polyoxometalates: From Platonic Solids to Antiretroviral Activity* (Eds.: M. T. Pope, A. Müller), Kluwer, Dordrecht (The Netherlands), **1994**; b) C. L. Hill, *Chem. Rev.* **1998**, *98*, special thematic issue, 1–390; c) *Polyoxometalate Chemistry: From Topology via self-Assembly to Applications* (Eds.: M. T. Pope, A. Müller), Kluwer, Dordrecht (The Netherlands), **2001**; d) *Polyoxometalate Chemistry for Nanocomposite Design* (Eds.: M. T. Pope, T. Yamase), Kluwer, Dordrecht (The Netherlands), **2002**; e) *Polyoxometalate Molecular Science* (Eds.: J. J. Borrás-Almenar, E. Coronado, A. Müller, M. T. Pope), Kluwer, Dordrecht (The Netherlands), **2003**; f) M. T. Pope in *Comprehensive Coordination Chemistry II* (Eds.: J. A. McCleverty, T. J. Meyer), Elsevier Ltd., Oxford (UK), **2004**.

[3] a) O. A. Kholdeeva, G. M. Maksimov, R. I. Maksimovskaya, L. A. Kovaleva, M. A. Fedotov, V. A. Grigoriev, C. L. Hill, *Inorg. Chem.* **2000**, *39*, 3828–3837; b) K. Nomiya, M. Takahashi, K. Ohsawa, J. A. Widegren, *J. Chem. Soc. Dalton Trans.* **2001**, 2872–2878; c) J. He, X. Wang, Y. Chen, J. Liu, N. Hu, H. Jia, *Inorg. Chem. Commun.* **2002**, *5*, 796–799; d) U. Kortz, S. S. Hamzeh, N. A. Nasser, *Chem. Eur. J.* **2003**, *9*, 2945–2952; e) F. Hussain, B. S. Bassil, L. Bi, M. Reicke, U. Kortz, *Angew. Chem.* **2004**, *116*, 3567–3571; *Angew. Chem. Int. Ed.* **2004**, *43*, 3485–3488; f) Y. Sakai, Y. Kitakoga, K. Hayashi, K. Yoza, K. Nomiya, *Eur. J. Inorg. Chem.* **2004**, 4646–4652; g) C. N. Kato, S. Negishi, K. Yoshida, K. Hayashi, K. Nomiya, *Appl. Catal. A* **2005**, *292*, 97–104; h) K. Hayashi, M. Takahashi, K. Nomiya, *Dalton Trans.* **2005**, 3751–3756; i) O. A. Kholdeeva, T. A. Trubitsina, M. N. Timofeeva, G. A. Maksimov, R. I. Maksimovskaya, V. A. Rogov, *J. Mol. Catal. A Chem.* **2005**, *232*, 173–178; j) O. A. Kholdeeva, T. A. Trubitsina, G. M. Maksimov, A. V. Golovin, R. I. Maksimovskaya, *Inorg. Chem.* **2005**, *44*, 1635–1642; k) R. J. Errington, S. S. Petkar, B. R. Horrocks, A. Houlton, L. H. Lie, S. N. Patole, *Angew. Chem.* **2005**, *117*, 1280–1283; *Angew. Chem. Int. Ed.* **2005**, *44*, 1254–1257; l) K. Hayashi, H. Murakami, K. Nomiya, *Inorg. Chem.* **2006**, *45*, 8078–8085; m) S. Shigeta, S. Mori, T. Yamase, N. Yamamoto, N. Yamamoto, *Biomed. Pharmacother.* **2006**, *60*, 211–219; n) Y. Goto, K. Kamata, K. Yamaguchi, K. Uehara, S. Hikichi, N. Mizuno, *Inorg. Chem.* **2006**, *45*, 2347–2356.

[4] O. A. Kholdeeva, R. I. Maksimovskaya, *J. Mol. Catal. A* **2007**, *262*, 7–24; O. A. Kholdeeva, *Top. Catal.* **2006**, *40*, 229–243.

[5] L.-Y. Qu, Q.-J. Shan, J. Gong, R.-Q. Lu, D.-R. Wang, *J. Chem. Soc. Dalton Trans.* **1997**, 4525–4528.

[6] X.-H. Wang, J.-F. Liu, Y.-G. Chen, Q. Liu, J.-T. Liu, M. T. Pope, *J. Chem. Soc. Dalton Trans.* **2000**, 1139–1141.

[7] R. Murugesan, P. Sami, T. Jeyabalan, A. Shunmugasundaram, *Trans. Met. Chem.* **1998**, *23*, 583–588.

[8] R. Murugesan, P. Sami, T. Jeyabalan, A. Shunmugasundaram, *Proc. Ind. Acad. Sci.* (Chem. Sci) **1995**, *107*, 1–10.

[9] O. A. Kholdeeva, T. A. Trubitsina, R. I. Maksimovskaya, A. V. Golovin, W. A. Neiwert, B. A. Kolesov, X. Lopez, J. M. Poblet, *Inorg. Chem.* **2004**, *43*, 2284–2292.

[10] P. Jeske, K. Wieghardt, B. Nuber, *Inorg. Chem.* **1994**, *33*, 47–53.

[11] U. Kortz, M. G. Savelieff, B. S. Bassil, M. H. Dickman, *Angew. Chem.* **2001**, *113*, 3488–3491; *Angew. Chem. Int. Ed. Engl.* **2001**, *40*, 3384–3386.

[12] U. Kortz, N. K. Al-Kassem, M. G. Savelieff, N. A. Al Kadi, M. Sadakane, *Inorg. Chem.* **2001**, *40*, 4742–4749.

[13] I. D. Brown, D. Altermatt, *Acta Crystallogr. Sect. B* **1985**, *41*, 244–247.

[14] F. Hussain, U. Kortz, R. J. Clark, *Inorg. Chem.* **2004**, *43*, 3237–3241.

[15] a) C. Tourné, A. Revel, G. Tourné, M. Vendrell, *C. R. Acad. Sc. Paris Ser. C.* **1973**, *277*, 643–645; b) C. Tourné, G. Tourné, *C. R. Acad. Sc. Paris Ser. C.* **1975**, *281*, 933–936.

[16] a) L. G. Detusheva, L. I. Kuznetsova, V. A. Likholobov, A. A. Vlasov, N. N. Boldyreva, S. G. Poryvaev, V. V. Malakhov, *Russ. J. Coord. Chem.* **1999**, *25*, 569–575; b) P. Mialane, J. Marrot, A. Mallard, G. Hervé, *Inorg. Chim. Acta* **2002**, *328*, 81–86.

[17] A. I. Vogel, *Quantitative Inorganic Analysis*, Longmans, London, **1960**.

[18] R. A. Sheldon, J. K. Kochi, *Metal-Catalyzed Oxidations of Organic Compounds*, New York, Academic Press, **1981**.

[19] R. Neumann, *Prog. Inorg. Chem.* **1998**, *47*, 317–370; R. Neumann, *Polyoxometalates as Catalysts for Oxidation with Hydrogen Peroxide and Molecular Oxygen in Transition Metals for Organic Synthesis, Vol. 2* (Eds.: M. Beller, C. Bolm), Wiley-VCH, Weinheim, 2nd ed., **2004**, pp. 415–426.

[20] C. Venturello, R. D'Aloisio, *J. Org. Chem.* **1988**, *53*, 1553–1557.

[21] A. C. Dengel, W. P. Griffith, B. C. Parkin, *J. Chem. Soc. Dalton Trans.* **1993**, 2683–2688.

[22] L. Salles, C. Aubry, R. Thouvenot, F. Robert, C. Doremieux-Morin, G. Chottard, H. Ledon, Y. Jeannin, J. M. Brégeault, *Inorg. Chem.* **1994**, *33*, 871–878.

[23] D. C. Duncan, R. C. Chambers, E. Hecht, C. L. Hill, *J. Am. Chem. Soc.* **1995**, *117*, 681–691.

[24] G. M. Maksimov, L. I. Kuznetsova, K. I. Matveev, R. I. Maksimovskaya, *Koord. Khim.* **1985**, *11*, 1353.

[25] T. Yamase, T. Ozeki, S. Motomura, *Bull. Chem. Soc. Jpn.* **1992**, *65*, 1453–1459.

[26] G. M. Sheldrick, SADABS, University of Göttingen, Göttingen (Germany), **1996**.

[27] B. Keita, F. Girard, L. Nadjo, R. Contant, J. Canny, M. Richet, *J. Electroanal. Chem.* **1999**, *478*, 76–82.

[28] B. Keita, R. Contant, E. Abdeljalil, F. Girard, L. Nadjo, *Electrochem. Commun.* **2000**, *2*, 295–300.

Received: January 10, 2007